Nanoscale

Mass Loading Effects in the Acoustic Vibrations of Gold Nanoplates

Journal:	*Nanoscale*
Manuscript ID	NR-COM-07-2019-005940.R1
Article Type:	Communication
Date Submitted by the Author:	20-Aug-2019
Complete List of Authors:	Devkota, Tuphan; University of Notre Dame, Department of Chemistry and Biochemistry Yu, Kuai; Shenzhen University, Hartland, Gregory; University of Notre Dame, Department of Chemistry and Biochemistry

Mass Loading Effects in the Acoustic Vibrations of Gold Nanoplates

Tuphan Devkota,[a] Kuai Yu,[b] and Gregory V. Hartland[a,1]

[a] *Department of Chemistry and Biochemistry, University of Notre Dame, Notre Dame, IN 46556, USA*

[b] *College of Electronic Science and Technology, Shenzhen University, Shenzhen, 518060, P. R. China*

Abstract: The breathing modes of single suspended gold nanoplates have been examined by transient absorption microscopy. These vibrational modes show very high quality factors which means that their frequencies can be accurately measured. Measurements performed before and after removing the organic layer that coats the as synthesized nanoplates show significant increases in frequency, which are consistent with removal of a few nm of organic material from the nanoplate surface. Experiments were also performed after depositing polymer beads on the sample. These measurements show a decrease in frequency in the region of the beads. This implies that adding a localized mass to the nanoplate hybridizes the vibrational normal modes, creating a new breathing mode which has a maximum amplitude at the bead. The nanoplate resonators have a mass sensing detection limit of ca. 10 attograms, which is comparable to the best results that have been achieved with plasmonic nanoparticles.

[1] Corresponding author; e-mail: ghartlan@nd.edu

Introduction:

Metal and semiconductor nanostructures display low frequency resonances in the THz to GHz range that correspond to their vibrational normal modes.[1-4] These acoustic vibrational modes can be studied by Raman spectroscopy,[5-6] and also appear in ultrafast transient absorption traces.[1-4] The frequencies of the acoustic modes can be accurately calculated using continuum mechanics if the size and shape of the nanostructure are known.[1-4] The damping of the vibrations in solid and liquid environments has also recently been investigated through both theory and experiment.[7-10] One of the potential applications of acoustic mode experiments is to use the nanostructures as ultra-small mass balances.[11-13] In these measurements the vibrational frequencies of the nanostucture are recorded before and after adsorption of a unknown object or amount of material, and the difference in frequency is used to determine the mass of the object/material. Transient absorption experiments on gold nanorods coated by Ag adlayers have demonstrated a detection limit of 40 attograms for ensemble measurements,[11] and approximately 10 attograms when single particles are interrogated.[12] However, much better detection limits have been achieved with nanoelectromechanical devices (NEMs), which typically employ the flexural modes of semiconductor nanobeams for mass sensing.[14-22]

In principle there are several advantages of using the acoustic vibrational modes metal or semiconductor nanostructures for mass sensing compared to NEMs devices. First, the acoustic modes can be addressed optically,[1-6] so that the measurements do not require complex fabrication to actuate the device and read out the signal. Second, the modes that are interrogated in the optical measurements (primarily breathing modes) have much higher frequencies than the flexural modes of beams. This implies smaller effective masses, which can translate into a higher mass sensitivity.[23-24] The major disadvantage of using the acoustic vibrational modes of nanostructures

for mass sensing is that they have lower quality factors compared to what has been achieved for the flexural modes of nanobeams, or the drum modes of membranes,[14-24] which limits the sensitivity of the measurement.

The quality factors of the acoustic modes of nanostructures are determined by internal relaxation and energy transfer to the environment.[2-4] The environmental part is dominated by radiation of sound waves into the surrounding medium.[10, 25-26] This decay pathway can be blocked by suspending the nanostructures over trenches,[27] or by placing them on substrates with low acoustic impedances, such as lacey carbon grids.[28] For gold nanowires the increase in quality factor for suspended nanowires compared to supported nanowires is modest, indicating that these materials suffer strong internal damping.[10, 29-30] In contrast, much larger improvements in the quality factor were observed for chemically synthesized gold nanoplates on lacey carbon grids.[28] For these samples the quality factors for the thickness vibration approach ~200. This was exploited in Ref. [[28]] to examine vibrational coupling between nanoplates. In this communication we investigate whether the high quality factors for the nanoplates allow mass sensing measurements. This is a complex question for these materials because the large lateral sizes of the nanoplates (several microns) means that any adsorbed material makes a small overall contribution to the total mass.

Experimental Methods:

The gold nanoplates were synthesized using the procedure as described in Ref. [[31]]. 2 mL of the nanoplate solution was washed two times in DI water to remove excess surfactant before depositing onto a glass slide (#1, Electron Microscopy Services). Marked trenches were prepared on the slide by photolithography and reactive-ion etching. This allowed for repeated measurements

of the same nanoplate after different treatments. To deposit the nanoplates, 200 μL of the sample was drop cast on a slide and allowed to dry. The coverslip was then mounted on a piezoelectric stage in an inverted optical microscope for optical measurements. Only Au nanoplates which were suspended over the markers were examined in this paper.[31] To study the effect of removing the surfactant coating (CTAB), the samples were cleaned by an oxygen plasma (Harrick Plasma Cleaner, PDC-32G) for 20 minutes at high RF power. Polystyrene beads with 0.8 μm mean particle size (Millipore Sigma) were also used for mass loading experiments. To deposit the beads on the nanoplates 50 μL of the sample was diluted to 10 mL in DI water and sonicated for 5 min. 100 μL of the diluted solution was spin coated onto the glass slide with Au nanoplates.

The vibrational frequencies of single suspended nanoplates were measured using transient absorption microscopy.[32-34] These experiments were performed using a laser system based on a Coherent Chameleon Ultra-II Ti-Sapphire oscillator. The output of the laser was tuned to 720 nm, and the beam was split into two parts using a 90:10 beam splitter. The weaker portion was used as the pump and the stronger portion was sent to a Coherent Mira OPO to generate a 530 nm probe beam. The pump and probe beams were combined at a dichroic mirror and focused at the sample using a high NA oil immersion microscope objective (Olympus UPlanFLN, 100x NA = 1.30). The reflected beams were collected by the same microscope objective and sent to an avalanche photodiode (Hamamatsu C5331-11) for detection. Short pass filters were used to extinguish the pump before the detector. The pump beam was modulated at 400 kHz using an acousto-optic modulator (IntraAction Corp.), and the pump induced change in the reflected probe power was detected with a lock-in amplifier (Stanford Research Systems, SR844). Transient absorption traces were recorded by changing the timing between the pump and probe pulses with a mechanical delay line (Thorlabs DDS600). The typical powers used were 300 μW for the pump and 100 μW for the

probe before the microscope objective. White light images of the sample were recorded in both reflection and transmission mode with a Thorlabs CMOS camera.

Results and Discussion:

Figure 1(a) shows a transient absorption trace of a suspended Au nanoplate (only the modulated portion of the traces in presented here). A reflected light image of the nanoplate is shown in Figure 1(b), and the Fourier transform of the transient absorption trace is presented in Figure 1(c). In these experiments the rapid heating by the ultrafast pump laser pulse impulsively excites vibrational modes of the nanostructure that correlate with the expansion coordinate.[1-4] For nanoplates the thickness vibration is excited.[31, 35] Because the nanoplates in these experiments are crystalline with (111) surfaces,[31] the motion for the thickness vibration is along the <111> direction of the lattice.[35] The frequency of this breathing mode vibration is therefore given by

$$\nu_{br} = \frac{c_L^{111}}{2h} \quad (1)$$

where c_L^{111} is the longitudinal speed of sound along the <111> lattice direction, and h is the plate thickness.[13, 35-36] For a cubic crystal c_L^{111} is given by $c_L^{111} = \sqrt{\left(C_{11} + 4(C_{44} - C_s')/3\right)/\rho}$ where $C_s' = (C_{11} - C_{12})/2$.[37] Using the single crystal elastic constant data for Au in Ref. [38] gives c_L^{111} = 3420 m/s. Thus, the ν_{br} = 41.3 ± 0.2 GHz vibrational frequency for the nanoplate in Figure 1(a) implies that this plate has a thickness of 41.4 ± 0.2 nm. Note that the nanoplates in these experiments are very uniform. Measurements at different positions yield frequencies that are identical within the resolution of the experiments (0.2 GHz). This can be seen in the vibrational spectra presented in Figure 2 below. However, there are large differences in vibrational frequencies between different nanoplates, due to polydispersity in the thickness dimension for the sample.[28, 31, 35]

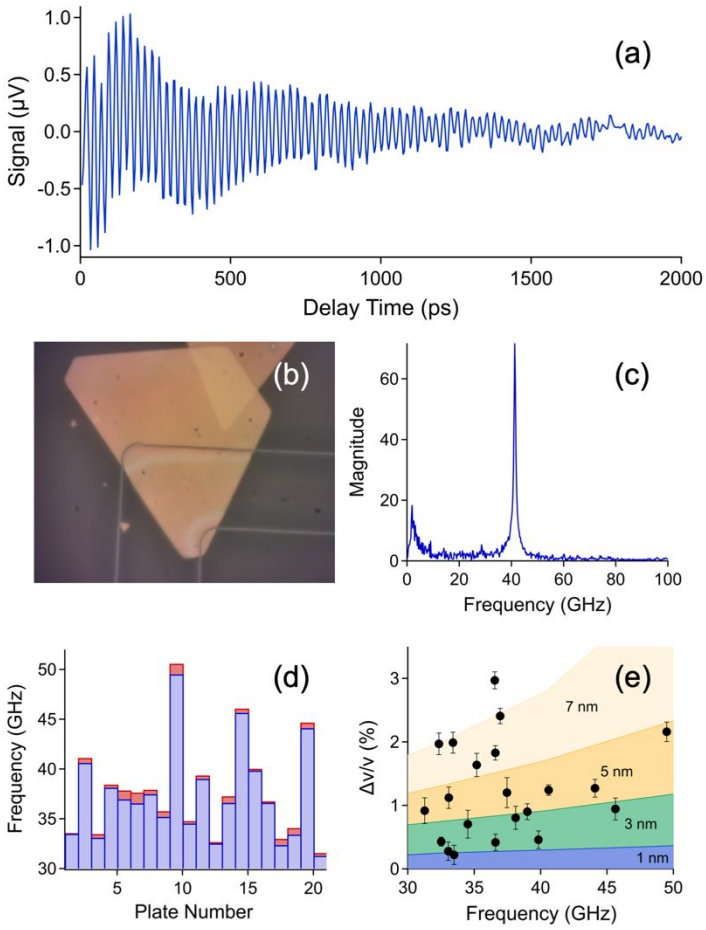

Figure1: (a) Transient absorption trace for a suspended Au nanoplate after subtraction of the background. (b) A scattered light image of the nanoplate and (c) the Fourier transform of the trace in panel (a). (d) The vibrational frequencies of different Au nanoplates before (blue bars) and after (red bars) plasma cleaning. (e) Relative percentage change in the vibrational frequencies of the nanoplates after plasma cleaning. The lines show calculations of the expected change in frequency for different thicknesses of the organic layer.

The vibrational quality factors for the suspended nanoplates are typically over 100, which is amongst the highest that have been recorded to date for metal nanostructures.[25, 28] This allows accurate measurements of the vibrational frequencies and, thus, potentially changes in frequency from mass loading effects.[13, 36, 39-40] Figure 1(d) shows the vibrational frequencies of the different nanoplates investigated in this study before (blue bars) and after (red bars) cleaning in an oxygen plasma to remove the organic material on the nanoplate surfaces. The nanoplates show consistently higher vibrational frequencies after plasma cleaning. The relative change in vibrational frequency $\Delta\nu/\nu$ for the different nanoplates is plotted versus frequency in Figure 1(e). The changes in vibrational frequency reach up to 3%, with an average value of $\Delta\nu/\nu = 1.2 \pm 0.8$ % (error equals standard deviation).

To understand the results in Figure 1 finite element simulations were performed for the vibrational normal modes of Au nanoplates with and without a layer of organic molecules at their surface. The simulations were performed in COMSOL Multiphysics (ver. 5.3) using the Solid Mechanics physics module. A two-dimensional geometry was used for the simulations, which strictly corresponds to infinitely long nanostripes rather than nanoplates. The simulations were performed for 2 μm wide nanoplates with thicknesses of 30 nm, 40 nm, 50 nm and 60 nm, and different thickness organic layers. The organic layers were considered to cover both sides of the nanoplates. Note that for a 2 μm wide nanoplate the frequency for the breathing mode calculated by COMSOL is virtually identical to the frequency calculated through Equation (1). The results of the simulations are shown as the lines in Figure 1(e).

The calculations show that the relative frequency changes depend on both the thickness of the initial organic layer, and the thickness of the nanoplate. For a given thickness organic layer, larger values of $\Delta\nu/\nu$ are obtained for thinner plates (higher frequencies) because there is a larger

relative change in mass when the coating is removed. On the other hand, for a given thickness of nanoplate, $\Delta\nu/\nu$ increases approximately linearly with the thickness of organic layer for the 40 – 60 nm thick nanoplates, and super-linearly for the 30 nm plates. The majority of the experimental $\Delta\nu/\nu$ values correspond to removal of 1 – 5 nm of organic material from the surfaces of the nanoplates. This should be compared to the ~ 3 nm thickness for a CTAB bilayer.[41] The distribution of $\Delta\nu/\nu$ values observed in Figure 1(e) is attributed to two effects: (i) the presence of multilayers of CTAB on the as deposited nanoplates, which will lead to larger $\Delta\nu/\nu$ values compared to the value expected for a bilayer after cleaning. (ii) Incomplete removal of the organic layer by plasma cleaning, which will reduce $\Delta\nu/\nu$.

The detection limit in these experiments can be estimated from the error in $\Delta\nu/\nu$. The average error for the suspended nanoplates in Figure 1(e) is 0.15%. For a 40 GHz frequency, which is in the middle of the data range in Figure 1(e), this value corresponds to removal of a ~0.5 nm thick layer of organic material. In terms of mass per unit area, this detection limit is roughly an order of magnitude better than the recent measurements for Ag deposition on gold nanorods.[12] A sub-1 nm thickness detection limit was also reported in Ref. [12], but Ag is 10x denser than the organic material examined here. However, a better way of characterizing the performance of mass sensing devices is the absolute mass that can be detected, which depends on the size of the nanostructure. Modeling the nanoplates as equilateral triangles with an edge length of 5 μm (which is the approximate size in the camera images), a 0.5 nm thick organic layer corresponds to a mass of approximately 10 attograms. This is similar to the detection limit reported in Ref. [12].

To further explore the potential of the suspended nanoplates as mass sensors, experiments were performed on suspended gold nanoplates with adsorbed 0.8 μm diameter polystyrene beads. Optical images of nanoplates with adsorbed beads and Fourier transforms of the transient

absorption traces recorded at different positions on the nanoplates are presented in Figure 2. The spectra show measurements at three different positions where there are no beads (black, red and blue lines in Figs. 2(d) – (f)), and repeated measurements at a position where there are beads (yellow circles in Figs. 2(a) – (c), and green and gold lines in Figs. 2(d) – (f)). Note that as far as we can tell from the optical images, the beads do not move or reshape during the experiments. Each nanoplate shows a repeatable red-shift in vibrational frequency when the measurements are performed with polystyrene beads at the focus of the pump and probe laser beams. However, the magnitude of the shift is different for the different nanoplates.

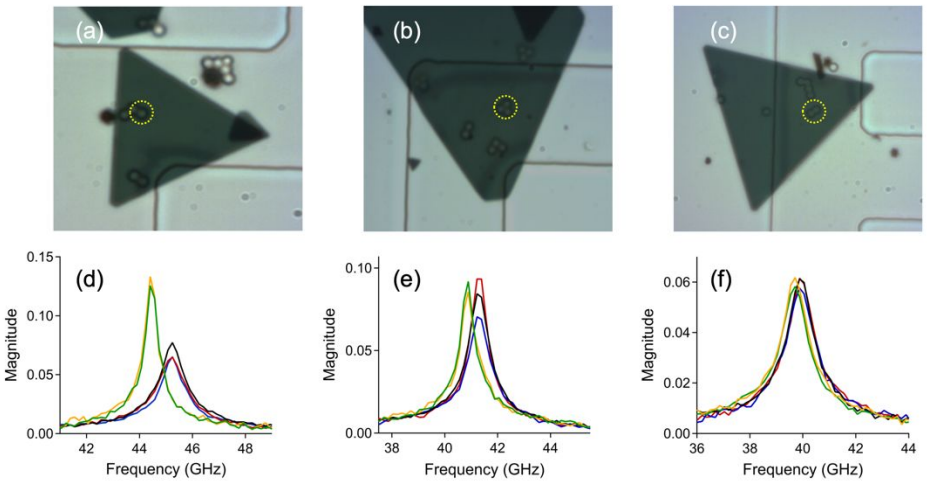

Figure 2: (a), (b) and (c): White light images of three different suspended Au nanoplates with adsorbed polystyrene beads. Transient absorption experiments were performed at positions corresponding to the beads (yellow circles) and at bead free regions. (d), (e) and (f): Vibrational spectra for the nanoplates showing a shift in the peak position to lower frequencies when the polystyrene beads are at the focus of the pump and probe beams. Green and gold lines are spectra recorded at the beads, and red, blue and black lines correspond to no beads.

There are several important points to note about the results in Figure 2. First, the observation of a spatially localized change in vibrational frequency due to mass loading is somewhat surprising. The thickness vibration of the nanoplate is a normal mode, whose amplitude should be distributed across the entire plate. Evidently adding a localized mass to the nanoplate hybridizes the vibrational normal modes, creating a new breathing mode which has a maximum amplitude at the particle. Second, different nanoplates show different responses to the added mass, with a maximum value of $\Delta\nu/\nu \approx 2\%$. There are several possible reasons for this. For example, the response of the nanostructure may depend on the position of the mass, as is the case for the flexural modes of beams.[18-22] It is also possible that the response depends on the contact between the beads and the resonator. Further experiments and finite element simulations are being conducted to investigate these effects, and to develop a protocol for determining the mass of the adsorbed nano-objects. In NEMs devices the mass and position of adsorbed particles can be determined by measuring the frequencies of two vibrational modes.[18-22] For the present system position can be determined optically, however, simulations will be needed to connect the frequency changes to mass. Note that recent studies of the vibrational modes of silicon nitride drums have shown that optical heating from adsorbed species (single gold nanoparticles or dye molecules) can change the vibrational frequencies of the system.[42] However, we do not think that this should be a big effect in our measurements, as the laser sources are not resonant to any transitions of the polymers.

Summary and Conclusions:

The high quality factors that can be achieved for suspended Au nanoplates means that their vibrational frequencies can be accurately measured in transient absorption experiments.

Measurements performed for nanoplates before and after plasma cleaning show changes in the vibrational frequencies that are consistent with removal of a 1 – 5 nm thick organic layer, which means that these materials are potential candidates for mass sensing experiments. However, a number of issues remain to be worked out. The data in Figure 2 shows that a few 0.8 μm diameter polystyrene beads can be detected in these measurements. The response is different for different nanostructures, which means that a better understanding of how the placement of adsorbed masses affects the response of the resonators is needed.

The current mass sensitivity for our resonators is ca. 10 attograms. This is similar to what has been achieved with the breathing modes of plasmonic nanoparticles, but is not competitive with NEMS devices.[14-24] A straightforward way to improve the response of the nanoplate resonators is to use structures with smaller lateral dimensions.[13] This will probably require the use of nanoplates supported on a lacey carbon grid,[28] or a similar low acoustic impedance substrates, rather than suspended nanoplates in this study. .

Acknowledgements: TD and GVH would like to acknowledge the support of the National Science Foundation through Award CHE-1502848. KY acknowledges the support from the National Natural Science Foundation of China (NSFC Grant No. 61705133).

ORCID: Tuphan Devkota: 0000-0002-0572-5874

Kuai Yu: 0000-0001-6138-0367

Gregory V. Hartland: 0000-0002-8650-6891

References:

1. Tchebotareva, A. L.; Ruijgrok, P. V.; Zijlstra, P.; Orrit, M., Probing the acoustic vibrations of single metal nanoparticles by ultrashort laser pulses. *Laser Photon. Rev.* 2010, *4*, 581-597.
2. Hartland, G. V., Optical studies of dynamics in noble metal nanostructures. *Chem. Rev.* 2011, *111*, 3858-3887.
3. Crut, A.; Maioli, P.; Del Fatti, N.; Vallee, F., Acoustic vibrations of metal nano-objects: Time-domain investigations. *Phys. Rep.* 2015, *549*, 1-43.
4. Major, T. A.; Lo, S. S.; Yu, K.; Hartland, G. V., Time-resolved studies of the acoustic vibrational modes of metal and semiconductor nano-objects. *J. Phys. Chem. Lett.* 2014, *5*, 866-874.
5. Saviot, L.; Champagnon, B.; Duval, E.; Kudriavtsev, I. A.; Ekimov, A. I., Size dependence of acoustic and optical vibrational modes of CdSe nanocrystals in glasses. *J. Non-Cryst. Solids* 1996, *197*, 238-246.
6. Portales, H.; Saviot, L.; Duval, E.; Fujii, M.; Hayashi, S.; Del Fatti, N.; Vallee, F., Resonant Raman scattering by breathing modes of metal nanoparticles. *J. Chem. Phys.* 2001, *115*, 3444-3447.
7. Del Fatti, N.; Voisin, C.; Chevy, F.; Vallee, F.; Flytzanis, C., Coherent acoustic mode oscillation and damping in silver nanoparticles. *J. Chem. Phys.* 1999, *110*, 11484-11487.
8. Pelton, M.; Chakraborty, D.; Malachosky, E.; Guyot-Sionnest, P.; Sader, J. E., Viscoelastic flows in simple liquids generated by vibrating nanostructures. *Phys. Rev. Lett.* 2013, *111*, 244502.
9. Chakraborty, D.; Hartland, G. V.; Pelton, M.; Sader, J. E., When can the elastic properties of simple liquids be probed using high-frequency nanoparticle vibrations? *J. Phys. Chem. C* 2018, *122*, 13347-13353.
10. Devkota, T.; Chakraborty, D.; Yu, K.; Beane, G.; Sader, J.; Hartland, G. V., On the measurement of relaxation times of acoustic vibrations in metal nanowires. *Phys. Chem. Chem. Phys.* 2018, *20*, 17687-17693.
11. Fernandes, B. D.; Spuch-Calvar, M.; Baida, H.; Treguer-Delapierre, M.; Oberle, J.; Langot, P.; Burgin, J., Acoustic vibrations of Au nano-bipyramids and their modification under Ag deposition: A perspective for the development of nanobalances. *ACS Nano* 2013, *7*, 7630-7639.

12. Yu, K.; Sader, J. E.; Zijlstra, P.; Hong, M.; Xu, Q.-H.; Orrit, M., Probing Silver Deposition on Single Gold Nanorods by Their Acoustic Vibrations. *Nano Letters* 2014, *14*, 915-922.
13. Girard, A.; Saviot, L.; Pedetti, S.; Tessier, M. D.; Margueritat, J.; Gehan, H.; Mahler, B.; Dubertret, B.; Mermet, A., The mass load effect on the resonant acoustic frequencies of colloidal semiconductor nanoplatelets. *Nanoscale* 2016, *8*, 13251-13256.
14. Chiu, H.-Y.; Hung, P.; Postma, H. W. C.; Bockrath, M., Atomic-scale mass sensing using carbon nanotube resonators. *Nano Letters* 2008, *8*, 4342-4346.
15. Jensen, K.; Kim, K.; Zettl, A., An atomic-resolution nanomechanical mass sensor. *Nature Nanotechnology* 2008, *3*, 533-537.
16. Naik, A. K.; Hanay, M. S.; Hiebert, W. K.; Feng, X. L.; Roukes, M. L., Towards single-molecule nanomechanical mass spectrometry. *Nat. Nanotechnol.* 2009, *4*, 445-450.
17. Chaste, J.; Eichler, A.; Moser, J.; Ceballos, G.; Rurali, R.; Bachtold, A., A nanomechanical mass sensor with yoctogram resolution. *Nature Nanotechnology* 2012, *7*, 300-303.
18. Hanay, M. S.; Kelber, S.; Naik, A. K.; Chi, D.; Hentz, S.; Bullard, E. C.; Colinet, E.; Duraffourg, L.; Roukes, M. L., Single-protein nanomechanical mass spectrometry in real time. *Nature Nanotechnology* 2012, *7*, 602-608.
19. Sage, E.; Brenac, A.; Alava, T.; Morel, R.; Dupre, C.; Hanay, M. S.; Roukes, M. L.; Duraffourg, L.; Masselon, C.; Hentz, S., Neutral particle mass spectrometry with nanomechanical systems. *Nat. Commun.* 2015, *6*, 6482.
20. Malvar, O.; Ruz, J. J.; Kosaka, P. M.; Dominguez, C. M.; Gil-Santos, E.; Calleja, M.; Tamayo, J., Mass and stiffness spectrometry of nanoparticles and whole intact bacteria by multimode nanomechanical resonators. *Nat. Commun.* 2016, *7*, 13452.
21. Sage, E.; Sansa, M.; Fostner, S.; Defoort, M.; Gely, M.; Naik, A. K.; Morel, R.; Duraffourg, L.; Roukes, M. L.; Alava, T., et al., Single-particle mass spectrometry with arrays of frequency-addressed nanomechanical resonators. *Nat. Commun.* 2018, *9*, 3283.
22. Dominguez-Medina, S.; Fostner, S.; Defoort, M.; Sansa, M.; Stark, A. K.; Halim, M. A.; Vernhes, E.; Gely, M.; Jourdan, G.; Alava, T., et al., Neutral mass spectrometry of virus capsids above 100 megadaltons with nanomechanical resonators. *Science* 2018, *362*, 918-+.
23. Ekinci, K. L.; Roukes, M. L., Nanoelectromechanical systems. *Rev. Sci. Instrum.* 2005, *76*, 061101

24. Arlett, J. L.; Myers, E. B.; Roukes, M. L., Comparative Advantages of Mechanical Biosensors. *Nat. Nanotechnol.* 2011, *6*, 203-215.
25. Medeghini, F.; Crut, A.; Gandolfi, M.; Rossella, F.; Maioli, P.; Vallée, F.; Banfi, F.; Del Fatti, N., Controlling the quality factor of a single acoustic nanoresonator by tuning its morphology. *Nano Letters* 2018, *18*, 5159−5166.
26. Devkota, T.; Brown, B. S.; Beane, G.; Yu, K.; Hartland, G. V., Making waves: Radiation damping in metallic nanostructures. *J. Chem. Phys.* 2019, DOI: 10.1063/1.5117230.
27. Major, T. A.; Crut, A.; Gao, B.; Lo, S. S.; Fatti, N. D.; Vallee, F.; Hartland, G. V., Damping of the acoustic vibrations of a suspended gold nanowire in air and water environments. *Phys. Chem. Chem. Phys.* 2013, *15*, 4169-4176.
28. Wang, J.; Yu, K.; Yang, Y.; Hartland, G. V.; Sader, J. E.; Wang, G. P., Strong vibrational coupling in room temperature plasmonic resonators. *Nat. Commun.* 2019, *10*, 1527.
29. Yu, K.; Major, T. A.; Chakraborty, D.; Devadas, M. S.; Sader, J. E.; Hartland, G. V., Compressible viscoelastic liquid effects generated by the breathing modes of isolated metal nanowires. *Nano Letters* 2015, *15*, 3964-3970.
30. Ruijgrok, P. V.; Zijlstra, P.; Tchebotareva, A. L.; Orrit, M., Damping of acoustic vibrations of single gold nanoparticles optically trapped in water. *Nano Letters* 2012, *12*, 1063-1069.
31. Major, T. A.; Devadas, M. S.; Lo, S. S.; Hartland, G. V., Optical and dynamical properties of chemically synthesized gold nanoplates. *J. Phys. Chem. C* 2013, *117*, 1447-1452.
32. Beane, G.; Devkota, T.; Brown, B. S.; Hartland, G. V., Ultrafast measurements of the dynamics of single nanostructures: a review. *Rep. Prog. Phys.* 2019, *82*, 016401.
33. Zhu, T.; Snaider, J. M.; Yuan, L.; Huang, L. B., Ultrafast dynamic microscopy of carrier and exciton transport. *Ann. Rev. Phys. Chem.* 2019, *70*, 219-244.
34. Fischer, M. C.; Wilson, J. W.; Robles, F. E.; Warren, W. S., Invited Review Article: Pump-probe microscopy. *Rev. Sci. Instrum.* 2016, *87*, 031101
35. Fedou, J.; Viarbitskaya, S.; Marty, R.; Sharma, J.; Paillard, V.; Dujardin, E.; Arbouet, A., From patterned optical near-fields to high symmetry acoustic vibrations in gold crystalline platelets. *Phys. Chem. Chem. Phys.* 2013, *15*, 4205-4213.
36. Girard, A.; Margueritat, J.; Saviot, L.; Machon, D.; Mahler, B.; Tessier, M. D.; Pedetti, S.; Dubertret, B.; Gehan, H.; Jeanneau, E., et al., Environmental effects on the natural vibrations of nanoplatelets: a high pressure study. *Nanoscale* 2017, *9*, 6551-6557.

37. Kim, K. Y.; Sachse, W.; Every, A. G., On the determination of sound speeds in cubic-crystals and isotropic media using a broad-band ultrasonic point-source point-receiver method. *J. Acoust. Soc. Am.* 1993, *93*, 1393-1406.
38. Simmons, G.; Wang, H., *Single crystal elastic constants and calculated aggregate properties: A handbook*; The MIT Press: Cambridge, MA, 1971.
39. Lee, E. M. Y.; Mork, A. J.; Willard, A. P.; Tisdale, W. A., Including surface ligand effects in continuum elastic models of nanocrystal vibrations. *J. Chem. Phys.* 2017, *147*, 044711.
40. Mork, A. J.; Lee, E. M. Y.; Dahod, N. S.; Willard, A. P.; Tisdale, W. A., Modulation of low-frequency acoustic vibrations in semiconductor nanocrystals through choice of surface ligand. *J. Phys. Chem. Lett.* 2016, *7*, 4213-4216.
41. Rutland, M. W.; Parker, J. L., Surface forces between silica surfaces in cationic surfactant solutions - adsorption and bilayer formation at normal and high pH. *Langmuir* 1994, *10*, 1110-1121.
42. Chien, M. H.; Brameshuber, M.; Rossboth, B. K.; Schutz, G. J.; Schmid, S., Single-molecule optical absorption imaging by nanomechanical photothermal sensing. *Proc. Natl. Acad. Sci. U.S.A.* 2018, *115*, 11150-11155.

Changes in vibrational frequencies for Au nanoplates have been used for mass sensing with a detection limit of 10 attograms.